# Cyclic Versus Linear Isomers Produced by Reaction of the Methylidyne Radical (CH) with Small Unsaturated Hydrocarbons

*Fabien Goulay,*[1,†,‡] *Adam J. Trevitt,*[1,*] *Giovanni Meloni,*[2,**] *Talitha M. Selby,*[2] *David L. Osborn,*[2] *Craig A. Taatjes,*[2] *Luc Vereecken*[3] *and Stephen R. Leone*[1,‡]

[1] Departments of Chemistry and Physics, and Lawrence Berkeley National Laboratory, University of California, Berkeley, California 94720, USA

[2] Combustion Research Facility, Mail Stop 9055, Sandia National Laboratories, Livermore, California 94551-0969, USA

[3] Department of Chemistry, K. U. Leuven, Celestijnenlaan 200F, B-3001 Leuven, Belgium

[†]Present address: Combustion Research Facility, Mail Stop 9055, Sandia National Laboratories, Livermore, California 94551-0969, USA

*Present address: School of Chemistry, University of Wollongong, Wollongong, NSW, 2522, Australia

**Present address: Department of Chemistry, University of San Francisco, 2130 Fulton Street, San Francisco, California 94611, USA

[‡]Electronic mail: fgoulay@sandia.gov; srl@berkeley.edu

***ABSTRACT***

The reactions of the methylidyne radical (CH) with ethylene, acetylene, allene, and methylacetylene are studied at room temperature using tunable vacuum ultraviolet (VUV) photoionization and time-resolved mass spectrometry. The CH radicals are prepared by 248 nm multiphoton photolysis of $CHBr_3$ at 298 K and react with the selected hydrocarbon in a helium gas flow. Analysis of photoionization efficiency versus VUV photon wavelength permits isomer-specific detection of the reaction products and allows estimation of the reaction product branching ratios. The reactions proceed by either CH insertion or addition followed by H atom elimination from the intermediate adduct. In the CH + $C_2H_4$ reaction the $C_3H_5$ intermediate decays by H atom loss to yield 70(±8)% allene, 30(±8)% methylacetylene and less than 10% cyclopropene, in agreement with previous RRKM results. In the CH + acetylene reaction, detection of mainly the cyclic $C_3H_2$ isomer is contrary to a previous RRKM calculation that predicted linear triplet propargylene to be 90% of the total H-atom co-products. High-level CBS-APNO quantum calculations and RRKM calculation for the CH + $C_2H_2$ reaction presented in this manuscript predict a higher contribution of the cyclic $C_3H_2$ (27.0%) versus triplet propargylene (63.5%) than these earlier predictions. Extensive calculations on the $C_3H_3$ and $C_3H_2D$ system combined with experimental isotope ratios for the CD + $C_2H_2$ reaction indicate that H-atom assisted isomerization in the present experiments is responsible for the discrepancy between the RRKM calculations and the experimental results. Cyclic isomers are also found to represent 30(±6)% of the detected products in the case of CH + methylacetylene, together with 33(±6)% 1,2,3-butatriene and 37(±6)% vinylacetylene. The CH + allene reaction gives 23(±5)% 1,2,3-butatriene and 77(±5)% vinylacetylene, whereas cyclic isomers are produced below the detection limit in this reaction. The reaction exit channels deduced by comparing the product distributions for the aforementioned reactions are discussed in detail.

## 1. Introduction

Small cyclic unsaturated hydrocarbons such as c-$C_3H$, c-$C_3H_2$, c-$C_3H_3$, and c-$C_4H_4$ are of great interest for the chemistry of carbon-rich gas-phase environments[1-6] and have been the subject of numerous theoretical and experimental investigations.[7-28] These cyclic molecules are believed to be vital intermediates in the chemical schemes leading to the formation of large carbon-containing molecules such as polycyclic aromatic hydrocarbons in combustion flames, the interstellar environment, and extraterrestrial atmospheres such as on a moon of Saturn, Titan. Because the linear and cyclic isomeric structures have different reactivities, the chemistry of gas phase environments in which these species are present is dependent on the relative abundance of each structure. Although the spectroscopic properties and the thermodynamics of the linear and cyclic forms have been studied, there remains a paucity of studies concerning the production of cyclic versus linear isomers, mostly due to the difficulty of detecting the structures of the reaction products.[29,30,31] Understanding the reaction mechanisms leading to the formation of cyclic and linear hydrocarbons is of major importance for the understanding of gas phase organic chemistry.

It is generally accepted that the formation of small cyclic hydrocarbons proceeds mostly by reaction of carbon atoms or small carbon radicals (such as CH, $C_2$, $C_3$) with small unsaturated hydrocarbons such as acetylene ($C_2H_2$) and ethylene ($C_2H_4$).[2,18,29,32-39] The formation of these cyclic species is usually in competition with the formation of the linear isomers.[29,30] Computational techniques are commonly used to infer the relative branching fractions for the formation of the cyclic isomers versus the linear counterparts. These predictions need to be benchmarked against experimental branching fractions. However, as the size of the carbon chain increases, computational studies become increasingly difficult to perform. It is therefore necessary to be able to qualitatively and quantitatively measure and predict the formation of cyclic/linear isomers for a given chemical reaction. For that purpose, reactions with acetylene ($C_2H_2$) and ethylene ($C_2H_4$) can be considered as archetypal reactions that will help predict the formation of cyclic compounds in reactions involving larger alkyne and alkene compounds.

The CH radical was one of the first molecules detected in the interstellar medium,[40] where it plays a vital role in the gas phase chemistry. In hydrocarbon flames the CH radical is responsible for blue emission by fluorescence from the first excited state to the ground state.[41] The CH radical is also one of the most reactive carbon species due to the presence of one singly occupied and one vacant non-bonding molecular orbital localized on the C atom. CH reactions with unsaturated hydrocarbon species are often fast and proven to proceed via a barrierless entrance channel to form intermediates that rapidly dissociate.[42] However, there is still debate on the exact nature of the preferred reaction mechanisms. Three entrance channels are generally considered for reaction of the CH radical with an unsaturated hydrocarbon molecule: insertion into a C–H bond, addition onto a single carbon atom and cycloaddition onto the π-electron system. After formation, the fate of the initial intermediate is usually complicated and can lead, after H or $H_2$ elimination, to cyclic or linear isomers. Theoretical investigations based on the quantum mechanical calculation of the minimum energy pathway have tried to predict the formation of cyclic versus linear isomers for the reactions of the CH radical with ethylene and acetylene.[17-19] For both reactions, it is predicted that the linear isomers will be dominant for energetic and/or entropic reasons, aided by rapid isomerization of any cyclic reaction intermediate to the more stable linear isomer.[17-19] These theoretical predictions are in disagreement with experimental studies on the CH + $C_2H_2$ reaction by Boullart et al.[39] and the unimolecular dissociation of the propargyl radical ($C_3H_3$) by McCunn et al.,[43] both reporting cyclopropenylidene (c-$C_3H_2$) as the main product.

In this paper, we present direct product detection and isomer-specific identification for the gas phase reactions of the CH radical with acetylene (R1), ethylene (R2), allene (R3) and methylacetylene (R4) at room temperature by time-resolved vacuum ultraviolet ionization mass spectrometry.

$$CH(X^2\Pi) + HCCH \rightarrow l/c\text{-}C_3H_2 + H \quad (R1)$$

$$CH(X^2\Pi) + H_2CCH_2 \rightarrow l/c\text{-}C_3H_4 + H \quad (R2)$$

$$CH(X^2\Pi) + H_2C{=}C{=}CH_2 \rightarrow l/c\text{-}C_4H_4 + H \quad (R3)$$

$$CH(X^2\Pi) + H_3C{-}C{\equiv}CH \rightarrow l/c\text{-}C_4H_4 + H \quad (R4)$$

The experiments are performed utilizing a slow flow reactor coupled to a photoionization mass spectrometer that uses tunable synchrotron radiation from the Advanced Light Source (ALS) synchrotron to identify product isomers according to their differing ionization energies, within the experimental energy resolution (~40 meV). The product distributions for the reactions of CH and CD with acetylene are compared to RRKM calculations performed on high-level CBS-APNO potential energy surfaces. The contribution of H-assisted isomerization to the measured isomer distribution is discussed in detail based on calculated $C_3H_2/C_3HD$ + H/D reaction product branching ratios. The product distribution for the reaction of CH and ethylene is compared to previous experimental and theoretical work. Deuterated methylidyne radical (CD) is also used in order to further investigate the reaction mechanism of the methylidyne radical with ethylene. The study of the CH radical reactions with allene and methylacetylene, for which only kinetic rate coefficient data[44] and H-atom branching ratios [45] are available, allows a further investigation of the CH radical reactivity with unsaturated hydrocarbons. The importance of the experimental results for each reaction to the understanding of gas-phase environmental chemistry is also discussed.

## 2. Experimental section

**Apparatus.** The experiments are performed in a slow flow reactor coupled to a multiplexed photoionization mass spectrometer. A description of the apparatus has been given elsewhere[46,47] and only a brief overview will be presented here. The gas flow consists of small amounts of radical precursor ($1.5\times10^{13}$ $cm^{-3}$) and reactant molecules ($5.1\times10^{14}$ $cm^{-3}$) in a large excess of He buffer gas at typical pressures of 4 Torr (533.3 Pa) at room temperature (total density of $1.3\times10^{17}$ $cm^{-3}$). The total pressure can be varied from 2 Torr (266.6 Pa) to 8 Torr (1066.6 Pa). The purities of gases are as follows: He, 99.999%; bromoform, 99%; acetylene, 99.6 %, ethylene, 99%, methylacetylene, 99%, allene, 97%, $CDBr_3$, 99.5%. Acetone stabilizer present in the acetylene cylinder is removed by passing the gas through an activated carbon filter.

A uniform initial concentration of CH radicals is produced coaxially in the flow by 248 nm photolysis of bromoform using an unfocused beam of an excimer laser with a 4 Hz repetition rate. The photodissociation of bromoform at 248 nm occurs *via* successive absorption of several photons[48] and requires a relatively low photon density, as opposed to a simultaneous multiphoton process. Typical photolysis fluences inside the reaction flow tube are ~(10 – 25) mJ/cm$^2$ in a 20 ns pulse. Chemical reactions proceed uniformly along the length of the reactor as the irradiated gas moves down the tube. Gas is extracted from the flow tube through a 650 μm diameter pinhole in the side of the tube into a chamber at relatively low pressure, typically a few $\times 10^{-5}$ Torr ($1.3 \times 10^{-3}$ Pa). The effusive beam emerging from the pinhole is skimmed by a 1.5 mm diameter skimmer before entering a differentially-pumped ionization region.

The gas beam is crossed by synchrotron undulator radiation that has been dispersed by a 3 m monochromator at the Chemical Dynamics Beamline of the Advanced Light Source at Lawrence Berkeley National Laboratory. The quasi-continuous, tunable vacuum ultraviolet light from the synchrotron ionizes molecules in the ionization region of a miniature double-focusing magnetic-sector mass spectrometer of the Mattauch-Herzog geometry.[49] The resulting ions are accelerated, focused, and dispersed according to the square roots of their masses in a 0.94 Tesla magnetic field. All ions within a variable mass range of about a factor of 8 (e.g., m/z =14 to m/z = 112) strike the active area of a time- and position-sensitive microchannel plate detector with a delay-line anode.[50] The position on the detector (corresponding to m/z) and time of arrival with respect to the photodissociation laser are recorded for each ion. The experiment is repeated for 200 – 400 laser pulses and the data are summed. The photon energy of the synchrotron can be scanned during an acquisition yielding a series of time-resolved mass spectra at each photoionization energy. The photon energy and the energy resolution (40 meV for 600 μm exit slit width) are calibrated by measurement of known atomic resonances of Xe, absorption resonances of Ar, and narrow autoionization resonances in $O_2$.

Because the apparatus collects time- and photon energy-resolved mass spectra, a 3-dimensional data block is available for each experiment consisting of ion intensity as a function of mass-to-charge ratio, reaction time, and photon energy. The photoionization efficiency (PIE) curves are constructed by integrating the data versus photon energy first over the desired mass-to-charge ratio, then over a time window that corresponds to the production of the species of interest in the photolytically-initiated reaction. In the following discussion the total reaction time is considered to be the first 80 ms after the triggering of the laser. Background contributions are removed by subtraction of the signal taken in the 20 ms before the photodissociation laser is triggered. Finally, these background-subtracted signals at each photon energy are normalized for the VUV photon flux and assembled into the PIE spectrum.

**Computational Methodology.** The computational method used to obtain the Franck-Condon photoionization simulations has been described in detail by Meloni et al.[47] All the calculations are performed using the Gaussian 03 program package.[51] The composite CBS-APNO (Complete Basis Set) method of Peterson and coworkers[52,53] is employed to provide reliable energetics, which for a reference set of molecules are expected to be accurate to within 5 kJ $mol^{-1}$. Structural parameters, including bond lengths, harmonic vibrational frequencies, and force constants of $C_3H_2$, $C_3H_4$ and $C_4H_4$ species are optimized using the Becke three-parameter exchange functional with the Lee, Yang, and Parr correlation functional (B3LYP) method and all-electron 6-311+G** basis set. Adiabatic ionization energies (AIE) are calculated using the CBS-APNO composite method. The normal-mode frequencies and force constants are then employed in the Franck-Condon (FC) spectral simulation to predict the overall shape and onset of the PIE curves. The FC spectral simulation of the PIE curves is carried out by computation and integration of the photoelectron spectra using the PESCAL[54,55] program. The experimental spectra are identified partly on the basis of their agreement with theoretical ionization energies and FC simulations.

The potential energy surface of the CH + $C_2H_2$ reaction[56] was re-characterized at the CBS-APNO level of theory, where the Hartree-Fock wavenumbers were replaced by a QCISD/6-311G(d,p) vibrational analysis on QCISD geometries. The mono-deuterated $C_3H_2D$ potential energy surface (PES) was likewise

determined by vibrational analysis of the deuterated intermediates; the relative energies change slightly due to differences in ZPE correction. RRKM Master Equation (RRKM-ME) analysis were then carried out on this CBS-APNO surface; the kinetic methodology was discussed in detail earlier[17] and is described only briefly here. The energy-specific rate coefficients k(E) in the energy-grained ME were calculated using RRKM theory, based on the CBS-APNO//QCISD data, in a rigid rotor harmonic oscillator approximation. Barrierless reactions, including the exit channels towards l-$C_3H_2$+H and c-$C_3H_2$+H, were characterized by microcanonical optimization of the k(E) at each energy level. Collisional energy transfer was modeled using Troe's bi-exponential model. The resulting RRKM-ME was solved using the CSSPI method as implemented in the URESAM program.[57]

## 3. Results

All the hydrocarbons used in this work have very low absorption cross sections at 248 nm (~$1\times10^{-21}$ $cm^2$ or less),[58-60] such that in the following discussion the contributions of hydrocarbon photoproducts to the ion signal of interest are neglected. The absorption cross section of bromoform at 248 nm is $1.94\times10^{-18}$ $cm^2$.[48] A recent study[48] showed that the primary photodissociation process is the breaking of one C–Br bond to produce $CHBr_2$ + Br. The successive photodissociation of $CHBr_2$ by a second and third photon at 248 nm produces CH, Br, HBr, CBr, CHBr and $Br_2$. Reactions of the CHBr, $CHBr_2$ and CBr radical with the studied hydrocarbons might form molecules with high molecular masses (>80 amu). Dissociative photoionization of these brominated products could contribute to the ion signal at lower masses. However, the rate constants for reactions of radicals such as CBr with small unsaturated hydrocarbons are several orders of magnitude smaller at room temperature (<$10^{-12}$ $cm^3$ $molecule^{-1}$ $s^{-1}$),[61-63] than those for reactions of the CH radical.[44,64] Any contribution from dissociative ionization of brominated molecules can therefore be identified by inspection of the time trace of the species. Using this kinetic analysis, contribution from dissociative ionization of higher-mass species to the ion signal at various product masses has been identified only for the detection of $C_3H_3$ cations and is negligible in other cases.

Multiphoton dissociation of bromoform at 248 nm is likely to form non-negligible amounts of vibrationally excited CH radicals. Quenching to the vibrational ground state is achieved by non-reactive collisions with a buffer gas. However collisions with helium atoms do not efficiently quench CH(v=1). The quenching rate coefficient of CH(v=1) by nitrogen molecules at 298 K is $3.1\times10^{-11}$ $cm^3$ $molecule^{-1}$ $s^{-1}$.[65] Adding 10% nitrogen to the main helium flow quenches the vibrationally excited CH radicals much faster than the characteristic time of any considered reactions, so that CH(v=1) contributions are negligible. Photoionization efficiency curves for the reaction of CH with acetylene have been recorded with 0%, 1% and 10% $N_2$ in the main flow. There were no significant changes observed in the final relative isomer distribution.

For a given reaction, the presence of several product isomers, each with different ionization energies, results in the appearance of several onset thresholds in the measured PIE curve. The presence of reaction products, within the experimental energy resolution, can then be verified using the ionization energies displayed in Table 1.

When multiple isomers contribute to the same PIE curve, the branching ratios for the production of each isomer are estimated by fitting the experimental PIE curve at a given mass with the sum of the absolute PIE curves of each of the identified products. The photoionization efficiency signals $S^E$ at photon energies $E$ are proportional to $\sigma^E$, which is the sum of the products of the isomeric photoionization cross section $\sigma_I^E$ and the molar fraction $x_I$ of the isomer $I$ (equations E1 and E2).

$$S^E \propto \sigma^E = \sum_I \sigma_I^E x_I \qquad \text{(E1)}$$

$$\sum_I x_I = 1 \qquad \text{(E2)}$$

When absolute photoionization cross sections are not available, estimated values are calculated using the semi-empirical model of Bobeldijk et al.[66] This model is assumed to be accurate to within 20% at

photon energies of 11.8 eV, which is far from the ionization threshold and far from any resonances for the hydrocarbons considered in the present work. Estimates of the photoionization cross sections for the overall photon energy range are then obtained by normalizing the predicted relative PIE curve (Franck-Condon photoionization simulations or integrated photoelectron spectra when available) to the estimated cross section at 11.8 eV. The branching ratio error bars are estimated as twice the standard deviation of the fit to the data using (E1) in order to take into account experimental uncertainties as well as uncertainty in the absolute photoionization cross-sections. In the following paragraphs, isomers produced by reaction of the CH radical with acetylene, ethylene, allene and methylacetylene are identified by analyzing the time dependent PIE curves.

### 3.1 Methylidyne reaction with acetylene

Triplet prop-2-enylidene (triplet propargylene), cyclopropenylidene (c-$C_3H_2$) and propadienylidene are the three expected H-atom co-products of the CH + acetylene reaction.[17] Within the measured photon-energy range (8.6 eV to 10.8 eV) these three $C_3H_2$ isomers are expected to be the only contributors to the ion signal at m/z=38. Figure 1 shows background-subtracted PIE curves of m/z=38 obtained from the CH + $C_2H_2$ reaction, integrated (a) over the entire reaction time (0 – 80 ms) and (b) from 20 ms to 80 ms after the laser pulse. More reliable product identification is achieved by analyzing the experimental PIE curve integrated over smaller time ranges because of different reactivities of the product isomers.

Figure 2 shows m/z=38 signal produced in the reaction of CH with acetylene as a function of the reaction time, acquired at (a) 9.05 eV and (b) 9.4 eV photon energies, obtained by summing the results of 5000 laser pulses. At a photoionization energy of 9.05 eV only the triplet propargylene species (*AIE*=8.96 eV)[30] can contribute to the m/z=38 signal. At this energy, the time decay of the m/z=38 signal is fitted by a single exponential decay with a characteristic time of 5 ms. Within the experimental signal-to-noise ratio the kinetic trace can also be fitted using a second order decay. As a result of this rapid temporal decay, observed only when $E < 9.15$ eV, the signal-to-noise ratio of the m/z = 38 PIE curve can be improved by integrating the ion signal in the narrow range of 0 – 3 ms, as shown in the inset of Figure 1(a). In this

inset, a threshold at $E \sim 8.9$ eV, corresponding to the photoionization of triplet propargylene (*AIE*=8.96 eV), is more clearly apparent. At 9.4 eV both isomers, triplet propargylene and c-$C_3H_2$ (*AIE*=9.15 eV),[12] may contribute to the m/z=38 signal. After 20 ms of reaction time all the triplet propargylene has reacted and does not contribute to the ion signal (see Figure 2(a)). The dotted line in Figure 2(b) is a single exponential fit to the data starting 20 ms after the photolysis. The fit gives a time constant of 23 ms. The contribution of triplet propargylene to the PIE curve of m/z=38 can be removed by integrating the ion signal only over a time at least 20 ms after the triggering of the laser as shown in Figure 1(b). The solid line in Figure 1 is the calculated PIE curve of cyclopropenylidene[30] fitted to the experimental data. The predicted PIE curve fits reasonably well to the experimental data and establishes the presence of the cyclic isomer of $C_3H_2$. There is no evidence of the propadienylidene isomer (*AIE*=10.36 eV) and, within the signal-to-noise ratio, no additional photoionization threshold is detected at energies higher than 10.5 eV (not shown).

The relative abundance of the two detected $C_3H_2$ isomers can be evaluated by comparing the ion signal at photoionization energies above and below the ionization threshold of c-$C_3H_2$. The photoionization cross sections for the $C_3H_2$ isomers have not been measured. Based on the pseudo-empirical method of Bobeldijk et al.[66] the photoionization cross sections for c-$C_3H_2$ and the triplet propargylene at 11.8 eV photon energy are of the order of 20 Mb and 16 Mb respectively. Considering Franck-Condon factors calculated by Taatjes et al.[30] for both $C_3H_2$ isomers, the photoionization cross sections at an energy below 9.5 eV are within the same order of magnitude, triplet propargylene having the largest photoionization cross section. In this case the relative signal intensity for both isomers observed below 9.5 eV strongly suggests that c-$C_3H_2$ represents at least 90% of the total $C_3H_2$ species. The lower limits of the branching ratios are displayed in table 2 and compared to predicted branching ratios based on RRKM-ME calculations. The predominance of the c-$C_3H_2$ product found experimentally is in disagreement with earlier theoretical kinetic work,[17] which predicted triplet propargylene as the dominant product (~90%). Although the photoionization cross section for both isomers are not known it seems

unlikely that the branching ratio for formation of the c-$C_3H_2$ is as small as predicted by previous RRKM-ME calculations.

A re-characterization of the potential energy surface at the very high CBS-APNO level of theory found a PES that is essentially the same as at the B3LYP and CASPT2 levels or theory,[56] but where the triplet propargylene + H product lies 21 kJ $mol^{-1}$ higher in energy. This change is larger than the uncertainties estimated earlier for the B3LYP PES,[17] and decreases the predicted contribution of this exit channel. RRKM-ME calculations on the CH + $C_2H_2$ reaction using the CBS-APNO PES find a substantially higher contribution of c-$C_3H_2$ (27.0%) versus triplet propargylene (63.5%) compared to the earlier predictions, but still do not indicate the rigid, cyclic $C_3H_2$ isomer as the dominant exit channel in the CH + $C_2H_2$ reaction (see Table 3). Considering the general reliability of the CBS-APNO level of theory, it is unlikely that further improvements to the PES will result in a direct yield of c-$C_3H_2$ + H that is sufficiently dominant to reproduce the experimental isomer ratio. However, alternative c-$C_3H_2$ formation mechanisms must be considered in the experiment. Specifically, H-assisted isomerization of the triplet-propargylene to the more stable c-$C_3H_2$ is a probable source of c-$C_3H_2$ in the present experiment (direct isomerization of triplet-propargylene to c-$C_3H_2$ proceeds via a transition state lying 151.7 kJ $mol^{-1}$ above triplet-propargylene[67]). The $C_3H_3$ adduct is formed with considerably less internal energy in the HCCCH + H reaction than in the CH + $C_2H_2$ reaction, and it is reasonable to assume that the branching will increasingly favor the lowest-energy channel, forming c-$C_3H_2$ + H.

If H-assisted isomerization occurred in the reaction flow the observed decay of the triplet propargylene isomer (5 ms, see Figure 2) would be the sum of two contributions: isomerization to c-$C_3H_2$ and reaction with other species in the flow. Therefore 5 ms is a lower limit for the isomerization characteristic time. In the flow conditions, H atoms are mostly produced by reaction of the CH radical with acetylene leading to a H-atom density of the order of $1\times10^{12}$ $cm^{-3}$. In order to achieve triplet propargylene isomerization within 5 ms, the upper limit of the rate constant of the H-assisted reaction needs to be on the order of $2\times10^{-10}$ $cm^3$ $s^{-1}$. The order of magnitude of this rate coefficient is consistent

with a barrierless radical-atom recombination. Based purely on the kinetic traces it is not possible to distinguish between H-assisted isomerization and direct c-$C_3H_2$ production. Therefore the H-assisted isomerization of $C_3H_2$ isomers has also been investigated theoretically using the revised $C_3H_3$ PES.

The reaction of triplet propargylene with H-atoms is a barrierless radical-radical recombination reaction, with a calculated rate coefficient close to the collision limit; regeneration of the reactants was found to be negligible. The energetically most-favorable exit channel is formation of c-$C_3H_2$ + H, and RRKM-ME calculations find c-$C_3H_2$ as the main reaction product (> 90%). The reaction of c-$C_3H_2$ + H is calculated to be an order of magnitude slower than l-$C_3H_2$ + H, due to the more rigid transition state and the need to break the aromaticity in the c-$C_3H_2$ moiety. Other than a small fraction regenerating the reactants, the main fate of the reaction of c-$C_3H_2$ + H is the formation of thermalized $C_3H_3$, due to the low excess energies at 298 K, and the absence of lower-lying exit channels. Therefore, triplet propargylene formed in the CH + $C_2H_2$ reaction can readily be converted to c-$C_3H_2$ in the reaction mixture in the presence of H atoms. Assuming that both isomers are removed by other reactions (such as wall removal) with a pseudo-first-order rate constant of 40 $s^{-1}$, quantitative agreement with the observed $C_3H_2$ data traces is obtained using the RRKM-ME results (Table 3) together with variational transition state theory (VTST) estimates of the rate coefficients. A ratio of photoionization cross sections of $\sigma_{l\text{-}C_3H_2}/\sigma_{c\text{-}C_3H_2} = 1.4$ gives the best fit to the experimental data suggesting at most a minor difference between the photoionization cross sections of the two isomers.

Signal observed at m/z=39 ($C_3H_3$) may be due to the ionization of propargyl (*AIE*=8.67 eV) and cycloprop-2-enyl (*AIE*=6.6 eV) produced by the CH + $C_2H_2$ reaction and stabilized by collision with the buffer gas. Also, the calculated branching ratios displayed in Table 3 suggest that a considerable amount of stabilized $C_3H_3$ radical may be formed by reaction of $C_3H_2$ isomers with H atoms. As mentioned earlier, for energies above 9.5 eV substantial contribution from dissociative ionization of higher-mass species is observed at m/z=39. The small ion signal below 9 eV together with the low ionization energy of the

cyclic-$C_3H_3$ isomer (*AIE*=6.6 eV) makes direct identification of the cyclic reaction intermediate difficult. However, additional evidence on the structure of the $C_3H_3$ reaction intermediate leading to the formation of the final H-atom co-products and the effect of the H-assisted isomerization can be obtained from the product isotopic ratio of the CD + $C_2H_2$ reaction products. Because there are two possible pathways producing a H atom and only one producing a D atom, the formation of cyclic-$C_3H_2D$ isomer along the reaction pathway will lead to hydrogen scrambling (H:D ratio of 2:1 in the absence of a kinetic isotope effect). The direct formation of propargyl would lead to a H:D ratio of 1:1.

Figure 3 shows a mass spectrum acquired from the CD + $C_2H_2$ reaction at 9.5 eV photon energy (accumulated with 1500 laser pulses). Comparing the area under the peaks at m/z = 39 ($C_3HD$) and m/z = 38 ($C_3H_2$) does result in a signal ratio of 2.04:1.00 in favor of the deuterated species. Signal at m/z = 40 corresponds to the $C_3H_2D$ cation. A mass spectrum was also recorded at 9.04 eV photon energy (2500 laser pulses), where only the acyclic isomer contributes to the $C_3H_2$ ion signal (see insert in Figure 3). In this case the signal levels at m/z = 39 and 38 are much weaker and the ratio of these signals around 3:1, again in favor of the $C_3HD$ product. This ratio is similar to that observed from the photodissociation of monodeuterated propargyl, $H_2CCCD$, in the molecular beam experiments of Deyerl et al.[68] The effect of deuteration on the branching ratios can be studied theoretically,

The reaction of deuterated methylidyne with acetylene, CD + $C_2H_2$, proceeds over the $C_3H_2D$ PES. For the task at hand, the most important impact of deuteration on this PES is the change in the vibrational wavenumbers and zero-point vibrational energies between $C_3H_2$ + D and $C_3HD$ + H exit channels. H-elimination is energetically more favorable by 5.8 kJ $mol^{-1}$ compared to D-elimination. Also, H-elimination is entropically favored due to formation of the less rigid $C_3HD$ coproduct, and the 2:1 H:D ratio in the $C_3H_2D$ intermediates. Chemically activated isomerization reactions of the $C_3H_2D$ intermediates are about 1 to 2 orders of magnitude faster than fragmentation into products, ensuring extensive scrambling of the H/D atoms. The RRKM-ME results show a 0.9:1 ratio of triplet propargylene versus c-$C_3H_2$ in the monodeuterated system (see Table 3), with a clear preference for $C_3HD$ formation of 3.7:1 and

2:1, respectively, for acyclic and cyclic isomers. However H/D-assisted isomerization combined with kinetic isotope effect might greatly affect the final isotopic distribution.

With a mixture of H and D atoms reacting with $C_3H_2$ and $C_3HD$ isomers, analysis of the effect of deuteration on the H-assisted isomerization of triplet propargylene to c-$C_3H_2$ is not straightforward; we limited ourselves here to the theoretical analysis of reactions involving nondeuterated and monodeuterated $C_3H_2D$ intermediates. As shown in Table 3, RRKM-ME calculations show a clear preference for deuterated $C_3HD$ products. Again, we find that (deuterated) triplet propargylene is readily converted to the cyclic isomer. For the $C_3HD$ + D and $C_3D_2$ + H reactions, one expects a similar preference for higher deuteration in the products, and again efficient conversion of triplet propargylene to cyclic isomers. Reaction of the cyclic isomers with H or D atoms is expected to be much slower than the equivalent reaction with triplet propargylene and to lead predominantly to thermalized $C_3H_3$/$C_3H_2D$ isomers (see Table 3).

Starting from a $C_3HD$:$C_3H_2$ ratio in favor of the deuterated isomer two effects must be considered to predict the final isotope ratio. On one hand, because the H atoms are formed by the CH + acetylene reaction, the isotopic ratio of D:H is necessarily the inverse of that of $C_3HD$:$C_3H_2$, and isomerization by reaction with the evolved H(D) atoms will tend to "undo" isotopic preferences and move the isotope ratios toward unity. On the other hand, the relatively strong preference of (deuterated) triplet propargylene to isomerize into c-$C_3HD$ rather than c-$C_3H_2$ in presence of a H or D atom could increase the $C_3HD$:$C_3H_2$ ratio. The prediction of the final isotope ratio is not simple as it depends on the branching ratios and rate coefficients of all the reactions displayed in Table 3. Nevertheless, an overall $C_3HD$:$C_3H_2$ isotope ratio of 2:1, in agreement with experiment, is obtained from a kinetic model including the reactions in Table 3, using VTST estimates for the rate coefficients and assuming a preference for higher deuteration in the products of $C_3HD$ + D.

### 3.2 Methylidyne reaction with ethylene

Cyclopropene, allene and methylacetylene are expected to be the only H-atom co-products of the CH + ethylene reaction.[19] Within the photon energy range employed in this study these three $C_3H_4$ isomers are likely to be the only contributors to the ion signal at m/z=40. Figure 4 shows the background-subtracted PIE curve of m/z=40 obtained from the CH/CD + $C_2H_4$ reaction, integrated over the full reaction time (0 – 80 ms). Figure 5(a) displays the data for reaction of the non-deuterated radical. Two photoionization thresholds are observed at around 9.67 eV and 10.4 eV. The first threshold corresponds to the ionization of either allene (A*IE*=9.69 eV) or cyclopropene (*AIE*=9.67 eV). As both isomers have similar ionization energies it is difficult to determine which isomer is responsible for the ion signal based on the threshold alone. The experimental PIE curve below 10.3 eV is compared to the known PIE curve of allene[69] (dashed line of Figure 4(a)) and to the integrated photoelectron spectrum of cyclopropene (dotted line in Figure 4(a)). Although allene and cyclopropene have a similar AIE the vertical ionization energy of cyclopropene is lower than that of allene, corresponding to a faster rising onset in the cyclopropene PIE compared to the allene PIE. The integrated photoelectron spectrum of cyclopropene is shifted by 0.05 eV to match the expected AIE of cyclopropene. It appears that within the (9.2-10.3) eV energy range the experimental data are best reproduced by the PIE curves of allene rather than cyclopropene. However, within the experimental uncertainty, cyclopropene could contribute up to 10% of the signal at mass 40 for energies lower than 10.3 eV. The second threshold is identified as the photoionization of methylacetylene (*IP*=10.36 eV). Branching ratios for the formation of the $C_3H_4$ isomers are obtained by fitting the experimental data with known and calculated PIE curves for each isomer.

The photoionization cross section of allene and methylacetylene have been measured by Cool at al.[69] up to 11.8 eV, but no data are available concerning the photoionization cross section of the cyclic $C_3H_4$ isomer. Using the model of Bobeldijk et al.[66] the relative integrated photoelectron spectrum of cyclopropene[70] is normalized to 20 Mb at 11.8 eV. Over the entire photon energy range the best fit to the experimental PIE curve at m/z=40 is obtained when adding 30(±8)% of the absolute PIE curve of

methylacetylene to 70(±8)% of the absolute PIE curve of allene (full line in Figure 4(a)). It is possible that cyclopropene could contribute <10% to the PIE signal. The experimental isomer product branching ratios are not pressure-dependent within the (2-6) Torr (133-800 Pa) pressure range. There is a possibility that the branching ratios could be affected by H-assisted isomerization of allene into the more stable methylacetylene. However, reaction of H atom with the stable singlet $C_3H_4$ products is much slower than the reaction with triplet propargylene. The isomerization rate coefficient of allene catalyzed by an H atom has been reported to be $2.7\times10^{-13}$ $cm^3$ $molecule^{-1}$ $s^{-1}$ at 300 K,[71] in accordance with recent theoretical work by Miller et al. on the $C_3H_5$ potential energy surface.[72] Under the present experimental conditions the H atoms are produced in the reaction of the CH radical with ethylene. Therefore the H atom density is expected to be no greater than the CH radical density (lower than $10^{12}$ $cm^{-3}$) such that the characteristic time for the isomerization reaction is more than one order of magnitude slower than the total experimental reaction time. The H-assisted isomerization can therefore be neglected in this case. The experimental branching ratios are displayed in Table 3 and compared to predicted branching ratios based on RRKM calculations using calculated $C_3H_5$ potential energy surfaces.[19]

Figure 4(b) shows the background-subtracted PIE curve of m/z=40 and m/z=41 obtained from the CD + ethylene reaction, integrated over the entire reaction time. The PIE curve at m/z=40 displays one onset at around 9.7 eV corresponding to the ionization energy of allene or cyclopropene. The PIE curve of m/z=40 can be fitted using 11(±10)% of the experimental absolute PIE curve of methylacetylene and 89(±10)% of the normalized calculated PIE of allene. The PIE curve at m/z=41 displays two onsets, one at ~9.7 eV, corresponding to the ionization energy of allene or cyclopropene, and the other at ~10.3 eV, corresponding to methylacetylene. Due to the small signal below 10.3 eV the identification of isomers is difficult. The experimental PIE curve at m/z=41 can be fitted using 33(±8)% of the experimental absolute PIE curve of allene and 67(±12)% of the experimental absolute PIE curve of methylacetylene as well as 35(±16)% of the integrated photoelectron spectrum of cyclopropene and 65(±8)% of the experimental absolute PIE curve of methylacetylene. Using either cyclopropene or allene lead to an equally good fit.

These results suggest that the reaction pathway leading to the formation of allene proceeds mainly via H-elimination when methylacetylene formation proceeds mainly via D-elimination.

### 3.3 Methylidyne reaction with allene and methylacetylene

The reaction of the CH radical with $C_3H_4$ isomers is expected to give products of the formula $C_4H_4$ together with the H-atom co-product. Based on their ionization energies and structures methylenecyclopropene, cyclobutadiene, vinylacetylene, and 1,2,3-butatriene are considered the only feasible contributors to the signal at m/z=52. Figure 5(a) shows the background-subtracted PIE curve of m/z=52 obtained from the CH + allene reaction, integrated over the entire measured reaction time (0-80 ms). Two onsets are observed around 9.2 eV and 9.5 eV, corresponding to photoionization of 1,2,3-butatriene (*AIE*=9.25 eV) and vinylacetylene (*AIE*=9.58 eV), respectively (see table 1). The solid line in Figure 5(a) represents the sum of the integrated photoelectron spectrum for 1,2,3-butatriene[73] and the measured PIE curve of vinylacetylene[74] fitted to the experimental data. The two vertical lines at 9.63 eV and 9.88 eV in Figure 5 indicate the known vibrational autoionization resonances of vinylacetylene,[74] confirming the presence of vinylacetylene. Within the experimental signal-to-noise ratio, no contribution from the cyclic-$C_4H_4$ isomers is observed (less than 1%) at energies below 9 eV.

Branching ratios for the formation of the $C_4H_4$ isomer from CH + allene are estimated. The absolute photoionization cross sections for $C_4H_4$ isomers have been experimentally determined only for vinylacetylene.[74] Using the Bobeldijk et al.[66] model the absolute photoionization cross section of 1,2,3-butatriene at 11.8 eV is estimated to be 24 Mb and is used to normalize the integrated photoelectron spectrum. The best fit to the experimental data is obtained using 23(±5)% of the estimated PIE curve of 1,2,3-butatriene and 77(±5)% of the measured PIE curve of vinylacetylene (solid line in Figure 5(a)).

Figure 5(b) shows the background-subtracted PIE curve of m/z=52 obtained from the CH + methylacetylene reaction, integrated over the entire measured reaction time (0-80 ms). Two main ionization thresholds are apparent, around 8.15 eV and 9.6 eV. As shown in Table 1, the two cyclic $C_4H_4$

isomers, methylenecyclopropene and cyclobutadiene, have ionization energies around 8.15 eV. At the experimental energy resolution it is not possible to differentiate between the ionization thresholds of these cyclic isomers. An attempt to identify the cyclic isomer by comparing the expected PIE curve of methylenecyclopropene (dotted line on Figure 2) and cyclobutadiene (dashed line Figure 8) is, within the limits of the signal to noise, inconclusive. The second observed ionization threshold around 9.6 eV corresponds to the ionization of vinylacetylene, as do the two vibrational auto-ionization resonances observed at 9.63 eV and 9.88 eV. No obvious threshold is detected for the ionization of 1,2,3-butatriene. However it is not possible to fit the experimental data using only the calculated PIE curve of the cyclic isomers and the measured PIE curve of vinylacetylene. A better fit of the experimental data is obtained by considering contributions from cyclobutadiene, 1,2,3-butatriene, and vinylacetylene. Thus estimates of the $C_4H_4$ –isomers branching ratios are obtained by fitting the experimental data with absolute PIE curves. The relative PIE curves of cyclobutadiene and 1,2,3-butatriene are normalized to the estimated cross sections at 11.8 eV (28 Mb and 24 Mb respectively). As both cyclic isomers have the same estimated cross section at 11.8 eV and a similar PIE curve, the use of either cyclobutadiene or methylenecyclopropene has no influence on the determination of the isomer branching ratios. The best fit to the experimental data is obtained using 30(±6)% of the estimated absolute PIE of cyclobutadiene/methylenecyclopropene, 33(±6)% of the estimated absolute PIE curve of 1,2,3-butatriene and 37(±6)% of the measured PIE curve of vinylacetylene. Table 3 lists the $C_4H_4$ isomers and branching ratios for the reactions of the CH radical with $C_3H_4$ isomers, allene and methylacetylene.

## 4. Discussion

### 4.1 Formation mechanism of $C_3H_2$ isomers by reaction of the CH radical with acetylene

Berman et al.[42] were the first to propose a mechanism for the reaction of the CH radical with acetylene. Since their early work several experimental and theoretical investigations have confirmed that the entrance channel is barrierless and leads to the formation of an excited intermediate of the formula $C_3H_3$.[17-19,43,64] Stabilization of $C_3H_3$ intermediates are usually not considered as important exit channels due to the high

exothermicity for the reaction intermediate formation. For the entrance channel, insertion of the CH radical into the C–H bond is considered to be unfavorable due to the large change of entropy compared to cycloaddition onto the π-electron system.[18] Kinetic isotope effect[20] measurements of rate coefficients for the CH/CD reaction with $C_2H_2/C_2D_2$ have shown almost no influence of the isotope substitution on the global reaction rate, suggesting that cycloaddition of the CH radical is the main entrance channel. Vereecken and Peeters[17] published a complete potential energy surface of the CH + $C_2H_2$ reaction. Using RRKM master-equation analysis, the authors provided a complete temperature and pressure dependence for the $C_3H_2$ product isomer distribution.[17] They concluded that no matter which entrance channel is dominant, propargyl will be the main reaction intermediate and that any cyclic $C_3H_3$ isomers formed are expected to isomerize to the more stable propargyl radical. This calculation also predicts triplet-propargylene as the main reaction product (around 90% at 298 K).[17] This reaction pathway was also found by Nguyen et al.[18] using a different level of theory. The present RRKM-ME calculations on the CH + $C_2H_2$ reaction using the CBS-APNO PES find a higher contribution of c-$C_3H_2$ (27.0%) versus l-$C_3H_2$ (63.5%) than the earlier predictions. This implies that cycloprop-2-enyl can directly dissociate to give c-$C_3H_2$ and a H atom or isomerize into the more stable linear propargyl radical. A schematic representation of the CH + $C_2H_2$ reaction pathways, based on the Vereecken and Peeters[17] quantum chemical characterization of the accessible region of the $C_3H_3$ potential energy surface, corrected for the CBS-APNO triplet propargylene + H energy is shown in Figure 6.

Although the experimental results show an isomeric ratio considerably different than that predicted by previous theory for the CH + $C_2H_2$ reaction, the combination of higher-level quantum calculations and RRKM-ME calculations of both the $C_3H_3$ and $C_3H_2D$ PES produce quantitative agreement with the observation of mainly c-$C_3H_2$ in our experiment. In addition to validating the reaction mechanism the present work shows the importance of H-assisted isomerization in gas-phase chemistry. The formation of $C_3H$ by $H_2$-elimination has been theoretically (see Table 3) and experimentally[39] shown to be possible. The

absence of any signal at mass 37 in the present experiments suggests that this channel is a minor one compared to the formation of $C_3H_2$ by H-elimination.

Reactions involving $C_3H_2$ isomers are included in the chemical scheme of combustion flames and Titan's atmosphere.[84,86] The reaction of the triplet-propargylene with the propargyl radical has been suggested as a possible pathway toward formation of the phenyl radical, which is an important intermediate for PAH formation.[30,86] In the present work, c-$C_3H_2$ is found to be produced by direct reaction of CH with acetylene and by H-assisted isomerization of initially formed triplet propargylene. If the reaction of CH with acetylene is the main source of $C_3H_2$ and H atoms are present in the surrounding, the triplet-propargylene density in gas phase environments may be low compared to the density of c-$C_3H_2$. Such results suggest that either triplet-propargylene is formed by another pathway or that c-$C_3H_2$ has a greater contribution to the carbon rich environment chemistry than its acyclic isomer.

**4.2 Formation mechanism of $C_3H_4$ isomers by reaction of the CH radical with ethylene**

The small kinetic isotope effects for the CH/CD + $C_2H_4$/$C_2D_4$ reactions measured by Thiesemann *et al.*[21] together with quantum chemical calculation by the same authors strongly suggest that the main entrance channel of the CH + ethylene reaction is the direct cycloaddition to form the cyclopropyl radical. McKee *et al.*[19] discussed the mechanism of this reaction and concluded that the fate of any cyclopropyl radical is likely to be conversion into the stable allyl radical. Direct elimination of the H atom on the central carbon from the allyl radical leads to the formation of allene. McKee et al. expect cyclopropene to be produced in a negligible amount. A 1,2-H shift on the deuterated allyl radical forms the 2-propenyl radical which can then decompose to either methylacetylene or allene, with a lower energy barrier toward methylacetylene formation.[75, 76] Direct H-elimination from the allyl radical is expected to be 10 times faster than the 1,2-H shift.[75] Detection of 70% allene as final product of the CH + ethylene reaction agrees well with this mechanism. The corresponding mechanism for reaction of the CD radical with ethylene is depicted in Figure 7. Cycloaddition followed by ring opening leads to deuterated allyl radical with the D atom on the central carbon. Formation of allene from this intermediate via D-elimination leads to non-

deuterated allene. After a 1,2-D shift, H-elimination from the -$CH_2$ group of the deuterated 2-propenyl radical, which is calculated to be more favorable than the H/D-elimination from the -$CH_2D$ group, leads to deuterated methylacetylene. The detection in the present study of mainly allene + D and methylacetylene-$d_1$ + H for the reaction of CD + $C_2H_4$ is consistent with this mechanism. Detection of a small amount of methylacetylene + D suggests that a 1,3-H shift can occur after formation of the allyl radical. Statistical H/D-elimination from the -$CH_2D$ group of the deuterated 2-propenyl radical leads to both deuterated and non-deuterated allene. The m/z=41 ion signal observed below 10.3 eV in Figure 5(b) is due to either deuterated cyclopropene formed by direct H-elimination from deuterated cyclopropyl or deuterated allene formed by statistical H/D elimination from the deuterated 2-propenyl radical. A H/D shift on the initial cyclopropyl radical would lead to a more complex isotopomer distribution.

McKee *et al.*[19] used the potential energy surfaces calculated by Davis *et al.*[75] and Deyerl *et al.*[76] to perform statistical calculations of the CH + ethylene product branching ratios. Table 2 compares the calculated values[19] to the experimental results obtained in the current study. Both the experimental data and theoretical isomeric distributions display a similar trend, with allene being the main reaction product followed by methylacetylene. Cyclopropene is produced either in negligible or very small amounts.

The ring opening of the excited cyclopropyl radical to the allyl radical is the most probable mechanism. Previous theoretical studies by Arnold and Carpenter[77] suggest that a small but finite cyclopropyl ring opening occurs through a transition state with a barrier of 90 kJ $mol^{-1}$. Intriguingly, there is experimental evidence of the cyclopropyl ring opening at 10 K,[78] where thermal energies are far below the calculated ring opening energy barrier. This discrepancy suggests that a channel other than that proposed by Arnold and Carpenter[77] may contribute to formation of allyl radical by ring opening of the cyclopropyl radical.

In Titan's atmospheric models, allene and methylacetylene are formed by reaction of the CH radical with ethylene.[84] Equal branching ratios are used for the production of both isomers, and allene is

considered to be converted into methylacetylene by H-assisted isomerization. These assumptions lead to an underestimation of the methylacetylene density compared to the in-situ measurements.[85] Incorporating the experimental 7:3 branching ratio for the CH + ethylene reaction favoring the formation of allene will lead to an even lower methylacetylene density. If the reaction of ethylene with the CH radical is the source of $C_3H_4$ isomers in Titan's atmosphere, a more efficient source of methylacetylene must be considered to explain the measured methylacetylene density.

### 4.3 Formation mechanism of $C_4H_4$ isomers by reaction of the CH radical with $C_3H_4$ isomers

To our knowledge there are no previous experimental or theoretical investigations of the H-atom co-products of reactions R3 and R4. Recently, Daugey *et al.*[44] measured the global rate coefficients for reaction of the CH radical with allene and methylacetylene from 77 K to 300 K. Both reactions are found to be fast and the rate coefficients are almost temperature independent. The authors of that study conclude that these two reactions are likely to proceed without any energy barrier above the reactant energy along the potential energy surface. Although their experiments do not give any information on the nature of the reaction products, Daugey *et al.* considered the two reactions to proceed *via* direct addition of the CH radical to a carbon atom (in contrast to the experimentally inferred mechanisms in the present work for CH + $C_2H_2$/$C_2H_4$). The energized reaction intermediate can then isomerize and/or dissociate to give the final products. Daugey et al.[44] also suggested 1,2,3-butatriene to be the main product of the CH reaction, with methylacetylene and 1,2,3-butatriene or vinylacetylene the main products of the CH reaction with allene. Similar mechanisms are proposed by Loison and Bergeat[45] based on experimental H-atom branching ratios and previous RRKM calculations. The experimental $C_4H_4$-isomer distribution produced by the CH + $C_3H_4$ reactions (see Table 3) shows that a more complex mechanism occurs and that cyclic isomers must be considered.

A complete $C_4H_5$ potential energy surface is yet to be generated. However Miller *et al.*[79] calculated a portion of the potential surface for the reaction of the vinyl radical with acetylene. Figure 8 shows a schematic view of the $C_4H_5$ potential energy surface calculated by Miller *et al.* together with available

exothermicities for formation of $C_4H_5$ isomers.[4,80,81] The exothermicities for cycloaddition of the CH radical to methylacetylene, forming a cycloprop-2-enyl-like intermediate (C) and to allene, forming a cyclopropyl-like intermediate (D), have been computed using the CBS-APNO method.[52,53] The total energy available for the reaction of CH with allene or methylacetylene differs by only 5.2 kJ $mol^{-1}$. Therefore, if the reaction mechanism along the $C_4H_5$ potential energy surface were governed by $C_4H_5$ isomerization to the most stable isomer, a similar $C_4H_4$-isomer product distribution would be expected for reaction with allene and methylacetylene. The detection of cyclic isomers for reaction (R4) but not (R3) suggests different reaction pathways and therefore different reaction intermediates for reactions (R3) and (R4).

For the CH + allene reaction, CH insertion into a C-H bond would form 1,2-butadiene-4-yl (B), which can then decompose to vinylacetylene, in accordance with Miller *et al.*,[79] or alternatively to 1,2,3-butatriene. However, on the basis of entropic arguments the addition entrance channels are more favorable. Addition of the CH radical to a terminal carbon atom followed by 2,3-H shift forms 1,3-butadien-1-yl (A), which could then decompose to vinylacetylene. Isomerization of 1,3-butadien-1-yl (A) to 1,2-butadien-4-yl (B) followed by H-elimination would result in the formation of vinylacetylene and 1,2,3-butatriene. As no cyclic products are detected it seems that any cyclic-$C_4H_5$ isomers formed by reaction of the CH radical with allene isomerize into a linear intermediate. This behavior is similar to that described for the reaction of CH with ethylene.

In the case of the CH + methylacetylene reaction the detection of cyclic compounds as the main reaction products suggests that cyclic $C_4H_5$ intermediates partially or totally decompose to cyclic $C_4H_4$ products. Within the experimental energy resolution it is not possible to estimate the relative contributions of methylenecyclopropene and cyclobutadiene to the ion signal. Direct cyclo-addition of the CH radical to the carbon triple bond would form a cycloprop-2-enyl-like intermediate (C). This mechanism is similar to the one inferred for the reaction of CH with acetylene. Formation of vinyl acetylene can occur by direct

insertion of the CH radical into a C-H bond of the methyl group similar to what has been observed and theoretically demonstrated for the reaction of CH + $CH_4$.[82]

In comparing the two above mentioned mechanisms for the reactions of the CH radical with isomers of $C_3H_4$ it appears that two types of cyclic intermediates, each formed by the most probable cycloaddition mechanism, may be considered, depending on the nature of the initial reactant. Reaction of the CH radical with allene leads to the formation of cyclopropyl-like intermediates by cycloaddition of the CH radical onto a carbon-carbon double bond, and reaction of the CH radical with methylacetylene leads to the formation of cycloprop-2-enyl-like intermediates by cycloaddition of the CH radical onto the carbon-carbon triple bond. In the case of cycloprop-2-enyl the C-C bond opposite the radical-bearing carbon is the shortest C-C bond,[4] whereas in cyclopropyl this corresponds to the longest C-C bond.[4,77] Due to the presence of a carbon-carbon double bond, the cycloprop-2-enyl displays a low barrier to pseudorotation through an allylic cyclo-intermediate providing a partial 3-electron delocalization. These different structural properties of these two kinds of cyclic species may lead to different behaviors regarding the opening of the carbon ring. Based on experimental data, it is reasonable to assume that in the case of CH + methylacetylene, the cycloprop-2-enyl-like intermediate tends to decompose to form cyclic final products. On the other hand, in the case of CH + allene, the cyclopropyl-like intermediate isomerizes into non-cyclic isomer.

Isomers of formula $C_4H_4$ are believed to be precursors of diacetylene ($C_4H_2$) in Titan's atmosphere. This molecule is a very important precursor for haze production.[83,84] The quantum yield for formation of diacetylene is likely to depend on the structure of the $C_4H_4$ isomers. The knowledge of the cyclic or linear structure of the $C_4H_4$ isomers will lead to a better understanding of diacetylene formation by photodissociation processes.

## 5. Conclusion

Direct detection of reaction products of CH radicals with small unsaturated hydrocarbons provides new insight into the mechanisms of these gas phase reactions. The reaction of the CH radical with acetylene has been studied both theoretically and experimentally. In our experiment, the detection of mainly cyclic $C_3H_2$ isomers is explained by the direct formation of both triplet propargylene and c-$C_3H_2$ followed by fast H-assisted isomerization of the triplet propargylene into c-$C_3H_2$. New CBS-APNO quantum chemical calculations and RRKM-ME computational kinetics show a branching ratio for direct formation of c-$C_3H_2$ by reaction of CH with acetylene greater than previously predicted, and can quantitatively reproduce the experimental observations.

The reaction of the CH radical with ethylene is found to produce mostly allene and methylacetylene with small amounts of cyclopropene. The deduced isomer distribution is consistent with theoretical calculations suggesting that the reaction proceeds *via* cyclo-addition followed by isomerization of the cyclic intermediate to allyl radical, which then decomposes to give the final linear products.

The reaction of the CH radical with isomers of $C_3H_4$ is found to give different final products depending on the structure of the initial reactant. Cyclic isomers are within the main reaction products in the case of CH + methylacetylene, whereas cyclic isomers are produced below the detection limit in case of CH + allene.

The experimental branching ratios for the studied reactions differ significantly from recent predictions[45] based only on previous RRKM calculations and H-atom branching ratios. This demonstrates the importance of isomer sensitive detection of reaction products. The branching ratios obtained in the present work may be used to model the chemical behavior of gas phase environments. Due to the large excess of available energy for all the studied reactions, decreasing the temperature should have only a small effect on the reaction branching ratios. At higher temperature however the branching ratios might differ from the one measured at room temperature. Although we did not observe a significant pressure

dependence of the branching ratios in the 2-8 Torr pressure range, the final product distributions might be different at much higher and lower pressure. The reaction mechanisms inferred from the present work may also be used to predict the isomeric structure of reaction products of the CH radical involved in the formation of larger unsaturated hydrocarbons such as benzene and PAHs. Further work, in the area of product detection and computational studies, is required to validate the fate of excited cyclic intermediates especially cycloprop-2-enyl-like intermediates.

**ACKNOWLEDGMENTS**

The support of personnel (F.G., A.J.T.) for this research by the National Aeronautics and Space Administration (grant NAGS-13339) is gratefully acknowledged. L.V. is indebted to the FWO-Vlaanderen for financial support. We thank Mr. Howard Johnsen for excellent technical support. Sandia authors and the instrumentation for this work are supported by the Division of Chemical Sciences, Geosciences, and Biosciences, the Office of Basic Energy Sciences, the U. S. Department of Energy. Sandia is a multi-program laboratory operated by Sandia Corporation, a Lockheed Martin Company, for the National Nuclear Security Administration under contract DE-AC04-94-AL85000. The Advanced Light Source and Chemical Sciences Division (S.R.L.) are supported by the Director, Office of Science, Office of Basic Energy Sciences of the U.S. Department of Energy under Contract No. DE-AC02-05CH11231 at Lawrence Berkeley National Laboratory.

**Supporting Information Available:** Complete ref. 49 This material is available free of charge via Internet at http://pubs.asc.org.

**References**


1. Lavallo, V.; Canac, Y.; Donnadieu, B.; Schoeller, W. W.; Bertrand, G. *Science* **2006,** 312, 722-724.

2. Kaiser, R. I.; Ochsenfeld, C.; HeadGordon, M.; Lee, Y. T.; Suits, A. G. *Science* **1996,** 274, 1508-1511.

3. Westmoreland, P. R.; Law, M. E.; Cool, T. A.; Wang, J.; McIlroy, A.; Taatjes, C. A.; Hansen, N. *Combust. Explo. Shock Waves* **2006,** 42, 672-677.

4. Wheeler, S. E.; Allen, W. D.; Schaefer, H. F. *J. Chem. Phys.* **2004,** 121, 8800-8813.

5. Thaddeus, P.; Vrtilek, J. M.; Gottlieb, C. A. *Astrophys. J.* **1985,** 299, L63-L66.

6. Kaiser, R. I. *Chem. Rev.* **2002,** 102, 1309-1358.

7. Mebel, A. M.; Jackson, W. M.; Chang, A. H. H.; Lin, S. H. *J. Am. Chem. Soc.* **1998,** 120, 5751-5763.

8. Stanton, J. F.; DePinto, J. T.; Seburg, R. A.; Hodges, J. A.; McMahon, R. J. *J. Am. Chem. Soc.* **1997,** 119, 429-430.

9. Seburg, R. A.; Depinto, J. T.; Patterson, E. V.; McMahon, R. J. *J. Am. Chem. Soc.* **1995,** 117, 835-836.

10. Herges, R.; Mebel, A. *J. Am. Chem. Soc.* **1994,** 116, 8229-8237.

11. Maier, G.; Preiss, T.; Reisenauer, H. P.; Hess, B. A.; Schaad, L. J. *J. Am. Chem. Soc.* **1994,** 116, 2014-2018.

12. Clauberg, H.; Minsek, D. W.; Chen, P. *J. Am. Chem. Soc.* **1992,** 114, 99-107.

13. Maier, G.; Reisenauer, H. P.; Schwab, W.; Carsky, P.; Hess, B. A.; Schaad, L. J. *J. Am. Chem. Soc.* **1987,** 109, 5183-5188.

14. Hehre, W. J.; Pople, J. A.; Lathan, W. A.; Radom, L.; Wasserman, E.; Wasserman, Z. R. *J. Am. Chem. Soc.* **1976,** 98, 4378-4383.

15. Skell, P. S.; Klebe, J. *J. Am. Chem. Soc.* **1960,** 82, 247-248.

16. Seburg, R. A.; Patterson, E. V.; Stanton, J. F.; McMahon, R. J. *J. Am. Chem. Soc*. **1997,** 119, 5847-5856.

17. Vereecken, L.; Peeters, J. *J. Phys. Chem. A* **1999,** 103, 5523-5533.

18. Nguyen, T. L.; Mebel, A. M.; Lin, S. H.; Kaiser, R. I. *J. Phys. Chem. A* **2001,** 105, 11549-11559.

19. McKee, K.; Blitz, M. A.; Hughes, K. J.; Pilling, M. J.; Qian, H. B.; Taylor, A.; Seakins, P. W. *J. Phys. Chem. A* **2003,** 107, 5710-5716.

20. Thiesemann, H.; MacNamara, J.; Taatjes, C. A. *J. Phys. Chem. A* **1997,** 101, 1881-1886.

21. Thiesemann, H.; Clifford, E. P.; Taatjes, C. A.; Klippenstein, S. J. *J. Phys. Chem. A* **2001,** 105, 5393-5401.

22. Kollmar, H. *J. Am. Chem. Soc*. **1980,** 102, 2617-2621.

23. Schulman, J. M.; Venanzi, T. J. *J. Am. Chem. Soc*. **1974,** 96, 4739-4747.

24. Buenker, R. J.; Peyerimhoff, S. d. *J. Am. Chem. Soc*. **1969,** 91, 4342-4346.

25. Maier, G. *Pure Appl. Chem*. **1986,** 58, 95-104.

26. Staley, S. W.; Norden, T. D. *J. Am. Chem. Soc*. **1989,** 111, 445-449.

27. Mebel, A. M.; Kaiser, R. I.; Lee, Y. T. *J. Am. Chem. Soc*. **2000,** 122, 1776-1788.

28. Sheeham, S. M.; Parsons, B. F.; Zhou, J.; Garand, E.; Yen, T. A.; Moore, D. T.; Neumark, D. M. *J. Chem. Phys*. **2008,** 128, 034301 1-13.

29. Costes, M.; Daugey, N.; Naulin, C.; Bergeat, A.; Leonori, F.; Segoloni, E.; Petrucci, R.; Balucani, N.; Casavecchia, P. *J. Chem. Soc., Faraday Trans*. **2006,** 133, 157-176.

30. Taatjes, C. A.; Klippenstein, S. J.; Hansen, N.; Miller, J. A.; Cool, T. A.; Wang, J.; Law, M. E.; Westmoreland, P. R. *Phys. Chem. Chem. Phys*. **2005,** 7, 806-813.

31. Kaiser, R. I.; Belau, L.; Leone, S. R.; Ahmed, M.; Wang, Y. M.; Braams, B. J.; Bowman, J. M. *Chem. phys. chem*. **2007,** 8, 1236-1239.

32. Cartechini, L.; Bergeat, A.; Capozza, G.; Casavecchia, P.; Volpi, G. G.; Geppert, W. D.; Naulin, C.; Costes, M. *J. Chem. Phys*. **2002,** 116, 5603-5611.

33. Clary, D. C.; Buonomo, E.; Sims, I. R.; Smith, I. W. M.; Geppert, W. D.; Naulin, C.; Costes, M.; Cartechini, L.; Casavecchia, P. *J. Phys. Chem. A* **2002,** 106, 5541-5552.

34. Geppert, W. D.; Naulin, C.; Costes, M. *Chem. Phys. Lett.* **2001,** 333, 51-56.

35. Kaiser, R. I.; Le, T. N.; Nguyen, T. L.; Mebel, A. M.; Balucani, N.; Lee, Y. T.; Stahl, F.; Schleyer, P. V.; Schaefer, H. F. *J. Chem. Soc., Faraday Trans.* **2001,** 119, 51-66.

36. Kaiser, R. I.; Mebel, A. M.; Lee, Y. T. *J. Chem. Phys.* **2001,** 114, 231-239.

37. Mebel, A. M.; Kaiser, R. I. *Chem. Phys. Lett.* **2002,** 360, 139-143.

38. Nguyen, T. L.; Mebel, A. M.; Kaiser, R. I. *J. Phys. Chem. A* **2001,** 105, 3284-3299.

39. Boullart, W.; Devriendt, W.; Borms, R.; Peeters, J. *J. Phys. Chem.* **1996,** 100, 998-1007.

40. Swings, P.; Rosenfeld, L. *Astrophys. J.* **1937,** 86, 483-486.

41. Bass, A. M.; Broida, H. P. *NBS Monogr* **1961**, 24-44.

42. Berman, M. R.; Fleming, J. W.; Harvey, A. B.; Lin, M. C. *Chem. Phys.* **1982,** 73, 27-33.

43. McCunn, L. R.; FitzPatrick, B. L.; Krisch, M. J.; Butler, L. J.; Liang, C. W.; Lin, J. J. *J. Chem. Phys.* **2006,** 125, 133306 1-11.

44. Daugey, N.; Caubet, P.; Retail, B.; Costes, M.; Bergeat, A.; Dorthe, G. *Phys. Chem. Chem. Phys.* **2005,** 7, 2921-2927.

45. Loison, J.-C.; Bergeat, A. *Phys. Chem. Chem. Phys.* **2008,** DOI: 10.1039/b812810c.

46. Goulay, F.; Osborn, D. L.; Taatjes, C. A.; Zou, P.; Meloni, G.; Leone, S. R. *Phys. Chem. Chem. Phys.* **2007,** 9, 4291-4300.

47. Meloni, G.; Zou, P.; Klippenstein, S. J.; Ahmed, M.; Leone, S. R.; Taatjes, C. A.; Osborn, D. L. *J. Am. Chem. Soc.* **2006,** 128, 13559-13567.

48. Zou, P.; Shu, J. N.; Sears, T. J.; Hall, G. E.; North, S. W. *J. Phys. Chem. A* **2004,** 108, 1482-1488.

49. Vallerga, J. V.; Siegmund, O. H. W. *Nucl. Instrum. Methods* **2000,** 442, 159-163.

50. Trott, W. M.; Blais, N. C.; Walters, E. A. *J. Chem. Phys.* **1978,** 69, 3150-3158.

51. Frisch, M. J. *et al. Gaussian 03, Revision C.02*, Gaussian, Inc: Wallingford CT, 2004.

52. Montgomery, J. A.; Ochterski, J. W.; Petersson, G. A. *J. Chem. Phys.* **1994,** 101, 5900-5909.

53. Ochterski, J. W.; Petersson, G. A.; Montgomery, J. A. *J. Chem. Phys.* **1996,** 104, 2598-2619.

54. Ervin, K. PESCAL Fortran program: 2004.

55. Ervin, K. M.; Ramond, T. M.; Davico, G. E.; Schwartz, R. L.; Casey, S. M.; Lineberger, W. C. *J. Phys. Chem. A* **2001,** 105, 10822-10831.

56. Vereecken, L.; Pierloot, K.; Peeters, J. *J. Chem. Phys.* **1998,** 108, 1068-1080.

57. Vereecken, L.; Huyberechts, G.; Peeters, J. *J. Chem. Phys.* **1997,** 106, 6564-6573.

58. Vattulainen, J.; Wallenius, L.; Stenberg, J.; Hernberg, R.; Linna, V. *Appl. Spect.* **1997,** 51, 1311-1315.

59. Rabalais, J. W.; McDonald, J. M.; Scherr, V.; McGlynn, S. P. *Chem. Rev.* **1971,** 71, 73-108.

60. Chen, F. Z.; Judge, D. L.; Wu, C. Y. R. *Chem. Phys.* **2000,** 260, 215-223.

61. Ruzsicska, B. P.; Jodhan, A.; Choi, H. K. J.; Strausz, O. P.; Bell, T. N. *J. Am. Chem. Soc.* **1983,** 105, 2489-2490.

62. James, F. C.; Ruzsicska, B.; McDaniel, R. S.; Dickson, R.; Strausz, O. P.; Bell, T. N. *Chem. Phys. Lett.* **1977,** 45, 449-453.

63. McDaniel, R. S.; Dickson, R.; James, F. C.; Strausz, O. P.; Bell, T. N. *Chem. Phys. Lett.* **1976,** 43, 130-134.

64. Canosa, A.; Sims, I. R.; Travers, D.; Smith, I. W. M.; Rowe, B. R. *Astron. Astroph* **1997,** 323, 644-651.

65. Herbert, L. B.; Sims, I. R.; Smith, I. W. M.; Stewart, D. W. A.; Symonds, A.; Canosa, A.; Rowe, B. R. *J. Phys. Chem.* **1996,** 100, 14928-14935.

66. Bobeldijk, M.; van der Zande, W. J.; Kistemaker, P. G. *Chem. Phys.* **1994,** 179, 125-130.

67. Mebel, A. M.; Kislov, V. V.; Hayashi, M. *J. Chem. Phys.* **2007,** 126, 204310 1-11.

68. Deyerl, H. J.; Fischer, I.; Chen, P. *J. Chem. Phys.* **1999,** 111, 3441-3448.

69. Cool, T. A.; Nakajima, K.; Mostefaoui, T. A.; Qi, F.; McIlroy, A.; Westmoreland, P. R.; Law, M. E.; Poisson, L.; Peterka, D. S.; Ahmed, M. *J. Chem. Phys.* **2003,** 119, 8356-8365.

70. Robin, M. B.; Wiberg, K. B.; Ellison, G. B.; Brundle, C. R.; Kuebler, N. A. *J. Chem. Phys.* **1972,** 57, 1758-1763.

71. Aleksandrov, E. N.; Arutyunov, I. V.; Dubrovina, I. V.; Kozlov, S. N. *Kinet. Catal.* **1980,** 21, 1323-1326.

72. Miller, J. A.; Senosiain, J. P.; Klippenstein, S. J.; Georgievskii, Y. *J. Phys. Chem. A* **2008,** 112, 9429-9438.

73. Brogli, F.; Heilbron.E; Klosterj.E; Schmelze.A; Manocha, A. S.; Pople, J. A.; Radom, L. *Chem. Phys.* **1974,** 4, 107-119.

74. Cool, T. A.; Wang, J.; Nakajima, K.; Taatjes, C. A.; McIlroy, A. *Inter. J. Mass Spect.* **2005,** 247, 18-27.

75. Davis, S. G.; Law, C. K.; Wang, H. *J. Phys. Chem. A* **1999,** 103, 5889-5899.

76. Deyerl, H. J.; Fischer, I.; Chen, P. *J. Chem. Phys.* **1999,** 110, 1450-1462.

77. Arnold, P. A.; Carpenter, B. K. *Chem. Phys. Lett.* **2000,** 328, 90-96.

78. Dong, F.; Davis, S.; Nesbitt, D. J. *J. Phys. Chem. A* **2006,** 110, 3059-3070.

79. Miller, J. A.; Klippenstein, S. J.; Robertson, S. H. *J. Phys. Chem. A* **2000,** 104, 7525-7536.

80. Parker, C. L.; Cooksy, A. L. *J. Phys. Chem. A* **1999,** 103, 2160-2169.

81. Krokidis, X.; Moriarty, N. W.; Lester, W. A.; Frenklach, M. *Inter. J. Chem. Kin.* **2001,** 33, 808-820.

82. Fleurat-Lessard, P.; Rayez, J. C.; Bergeat, A.; Loison, J. C. *Chem. Phys.* **2002,** 279, 87-99.

83. Lavvas, P. P.; Coustenis, A.; Vardavas, I. M. *Planet. Space. Sci.* **2008,** 56, 27-66.

84. Lavvas, P. P.; Coustenis, A.; Vardavas, I. M. *Planet. Space. Sci.* **2008,** 56, 67-99.

85. Parr, A. C.; Jason, A. J.; Stockbauer, R. *Inter. J. Mass Spect.* **1980,** 33, 243-251.

86. NIST Standard Reference Database Number 69, NIST Chemistry WebBook, National Institute of Standards and Technology, Gaithersburg MD, 20899 (http://webbook.nist.gov).

87. Kohn, D. W.; Chen, P. *J. Am. Chem. Soc*. **1993,** 115, 2844-2848.

88. Rosenstock, H. M.; McCulloh, K. E.; Lossing, F. P. *Inter. J. Mass Spect*. **1977,** 25, 327-341.

89. Hohlneicher, G.; Packschies, L.; Weber, J. *Phys. Chem. Chem. Phys*. **2007,** 9, 2517-2530.

**Table 1:** Adiabatic ionization energy (AIE) for the expected isomers produced by reaction of the CH radical with ethylene, acetylene, methylacetylene and allene.

| $C_3H_2$ isomers (Mass 38) | AIE (eV) | $C_3H_4$ isomers (Mass 40) | AIE (eV) | $C_4H_4$ isomers (Mass 52) | AIE (eV) |
|---|---|---|---|---|---|
| Prop-2-enylidene[30] (triplet propargylene) | 8.96 | Cyclopropene [85] | 9.67 | Methylenecyclopropene[26] | 8.15 |
| Cyclopropenylidene[12] (c-$C_3H_2$) | 9.15 | Allene[86] | 9.69 | Cyclobutadiene [87] | 8.16 |
| Propadienylidene[12] | 10.43 | Methylacetylene[86] | 10.36 | 1,2,3-butatriene[88] | 9.25 |
| | | | | Vinyl acetylene[88] | 9.58 |

**Table 2:** Estimated isomer distribution produced by reactions of the CH radical with acetylene, ethylene and $C_3H_4$ isomers. RRKM calculated branching ratios are also shown for the reaction of CH with ethylene.[19] The numbers between parentheses are the error bars reported as $2\sigma$.

| | | Experimental Branching ratios[a] | | RRKM-ME | |
|---|---|---|---|---|---|
| $CH + C_2H_2$ | triplet propargylene | <10% | | 89.9%[b] | 63.5%[a] |
| | Cyclopropenylidene | >90% | | 6.9%[b] | 27.0%[a] |
| | Propadienylidene | Not detected | | ≤3.2%[b] | ≤9.5%[a] |
| $CH + C_2H_4$ | Cyclopropene | 10(±10)% | | – | |
| | Allene | 70(±8)% | | 94%[c] | |
| | Methyacetylene | 30(±8)% | | 6%[c] | |
| $CH + C_3H_4$ | | CH + methylacetylene | CH + allene | Not available | |
| | Cyclic isomers | Not detected | 30(±6)% | | |
| | 1,2,3-butatriene | 23(±5)% | 33(±6)% | | |
| | Vinyl acetylene | 77(±5)% | 37(±6)% | | |

[a] Present work
[b] Results by Vereecken and Peeters[17] based on B3LYP-DFT PES
[c] Results by McKey *et al.*[19]

**Table 3:** RRKM-ME predicted product distributions for reactions on the $C_3H_3$ and $C_3H_2D$ CBS-APNO potential energy surfaces, for T = 298 K and P = 4 Torr.

| Reaction | l-$C_3H_2$+H/D | l-$C_3HD$+H | c-$C_3H_2$+H/D | c-$C_3HD$+H | Other products |
|---|---|---|---|---|---|
| $C_2H_2$ + CH [a] | 89.9 % | | 6.9 % | | 3.2 % [b] |
| $C_2H_2$ + CH | 63.5 % | | 27.0 % | | 9.5 % [b] |
| l-$C_3H_2$ + H | / | | 92.9% | | 7.1% [c] |
| c-$C_3H_2$ + H | < 0.1 % | | / | | > 99.9 % [c] |
| $C_2H_2$ + CD | 9.9 % | 37.2 % | 13.9 % | 28.2 % | 10.9 % [b] |
| l-$C_3H_2$ + D | / | 4.4 % | 24.5 % | 68.7 % | 2.4 % [b] |
| l-$C_3HD$ + H | 0.2 % | / | 24.2 % | 71.5 % | 4.1 % [c] |
| c-$C_3H_2$ + D | < 0.1 % | < 0.1 % | / | 3.5 % | 96.4 % [c] |
| c-$C_3HD$ + H | < 0.1 % | < 0.1 % | 0.1 % | / | 99.9 % [c] |

[a] Results by Vereecken et Peeters[17] based on B3LYP-DFT PES
[b] Predominantly $H_2CCC$+H and $C_3H$+$H_2$
[c] Predominantly thermalized $C_3H_3$

**Figure captions**

**Figure 1.** Photoionization efficiency curve of m/z=38 obtained by reaction of the CH radical with acetylene obtained (a) over the entire reaction time (0 – 80 ms) and (b) from 20 ms to 80 ms after the laser pulse. The inset shows the signal integrated over the first 3 ms following the triggering of the laser. The thick line is the Franck-Condon simulation[30] of cyclopropenylidene at 300 K fitted to the data.

**Figure 2.** Time dependent signal of m/z=38 obtained by reaction of the CH radical with acetylene. The signal of mass 38 has been integrated over 5000 laser pulses at (a) 9.05 eV and (b) 9.4 eV photon energy. The full line is a fit of the data taken at 9.05 eV assuming a single exponential decay. The dashed line is a fit of the data taken at 9.4 eV, 20 ms after the triggering of the laser, assuming a single exponential decay.

**Figure 3.** Mass spectrum acquired from the CD + $C_2H_2$ reaction at 9.5 eV photon energy (1500 laser shots). The inset shows the mass spectrum acquired from the same reaction at 9.05 eV photon energy (2500 laser shots).

**Figure 4.** Photoionization efficiency curve of m/z=40 (circles) and m/z=41 (triangles) obtained by reaction of the (a) CH radical and (b) CD radical with ethylene. In (a) the dotted line is the integrated photoelectron spectrum of cyclopropene and the dashed line is the experimental absolute PIE of allene at 300 K, each fitted to the data for energies below 10.3 eV. The full line is the fit of the experimental data using 70% of the absolute experimental PIE curve of allene and 30% of the absolute experimental PIE curve of methylacetylene. In (b) the dotted line is the fit to the experimental PIE curve of m/z=40 and corresponds to 89% of allene and 11% of methylacetylene. The dashed line is the fit to the experimental PIE curve of m/z=41 using 35% of the normalized integrated photoelectron spectrum of cyclopropene and 65% of the absolute experimental PIE curve of methylacetylene.

**Figure 5.** Photoionization efficiency curve of m/z=52 obtained by reaction of the CH radical with allene (a) and methylacetylene (b). The solid line in (a) is the fit of the experimental data using an estimated PIE curve of 1,2,3-butatriene (see text) and the absolute experimental PIE curve of pure vinyl-acetylene.[74] The

two vertical lines at 9.63 eV and 9.88 eV indicate the known vibrational autoionization resonances of vinylacetylene.[74] The best fit corresponds to 23% of 1,2,3-butatriene and 77% of vinylacetylene. In (b) the calculated Franck-Condon PIE curve of methylenecyclopropene (dashed line) and cyclobutadiene (dotted line) are superimposed to the experimental data. The solid line is the fit of the experimental data using calculated PIE curves of cyclobutadiene and 1,2,3-butatriene (see text) and absolute experimental PIE curve of pure vinylacetylene.[74] The best fit corresponds to 30% of cyclobutadiene, 33% of 1,2,3-butatriene and 37% of vinylacetylene.

**Figure 6.** Schematic of the $C_3H_3$ potential energy surface based on the calculations by Vereecken *et al.*,[17] corrected for the CBS-APNO triplet propargylene + H energy.

**Figure 7.** Likely mechanism for the formation of allene, propyne and cyclopropene and their deuterated isotopologs by cyclo-addition of the CD radical onto ethylene. The bold arrows indicate the expected favorable pathways due to either a higher entropy (direct D-elimination from allyl compared to 1,2-shift) or a lower energy (formation of methylacetylene from 2-propenyl compared to formation of allene) transition state.

**Figure 8.** Schematic of the $C_4H_5$ potential energy surface based on the calculation of Miller *et al.*[79] together with relative exothermicities for the formation of $C_4H_5$ and $C_4H_4$ isomers calculated using thermodynamic data of Wheeler *et al.*[4] and Hohlneicher *et al.*[89] The exothermicities of the cyclics species (C) and (D) are calculated using the CBS-APNO method (see text).

**Figure 1**

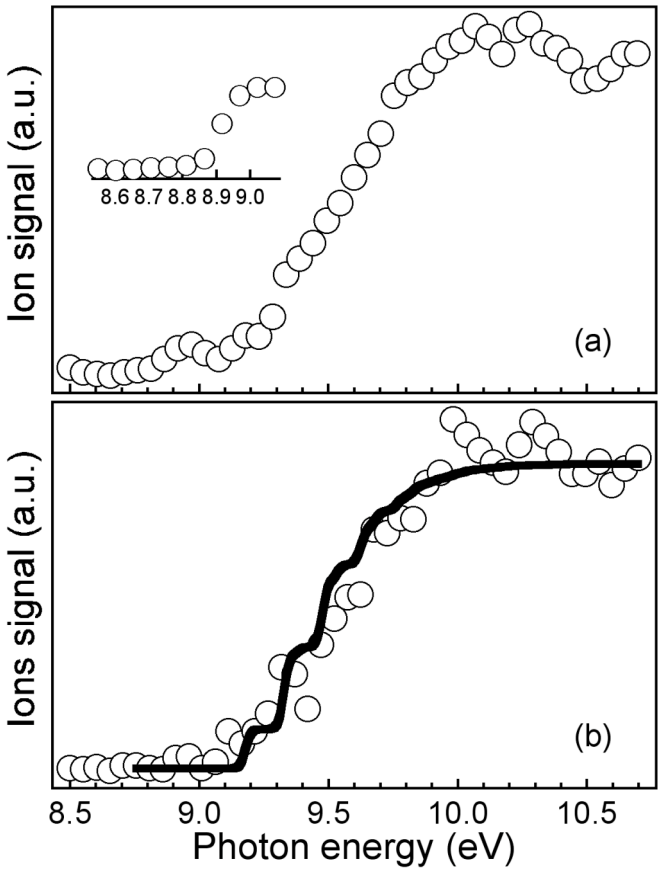
Ion signal (a.u.)
8.6 8.7 8.8 8.9 9.0
(a)
Ions signal (a.u.)
(b)
8.5
9.0
9.5
10.0
10.5
Photon energy (eV)

**Figure 2**

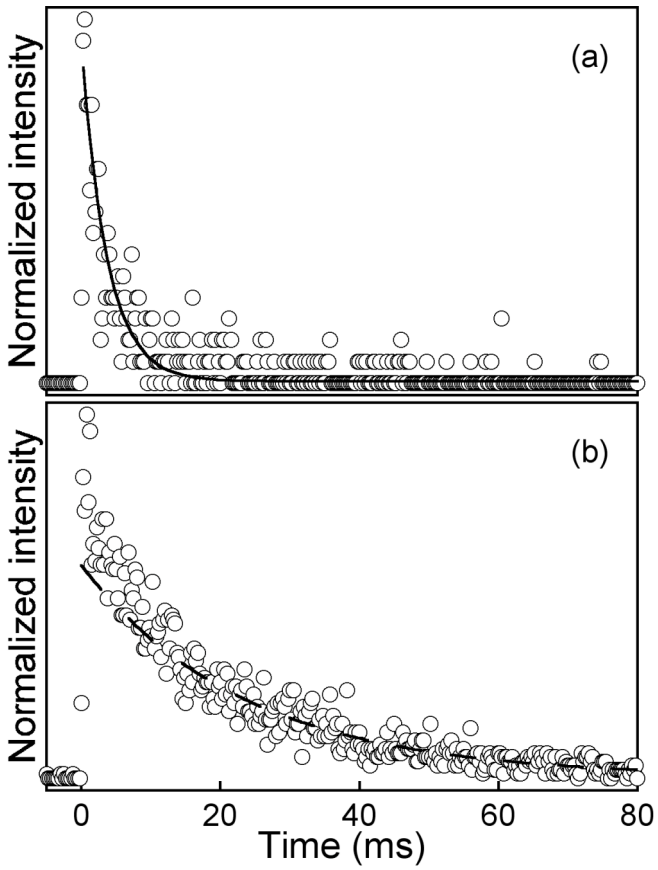
(a)
Normalized intensity
(b)
Normalized intensity
0
20
40
60
80
Time (ms)

**Figure 3**

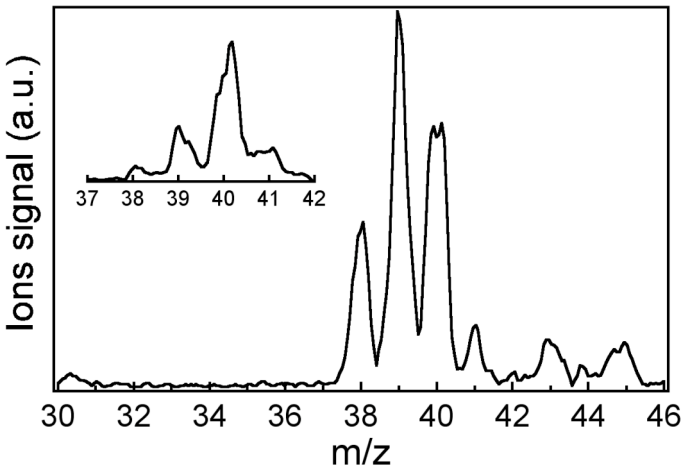

**Figure 4**

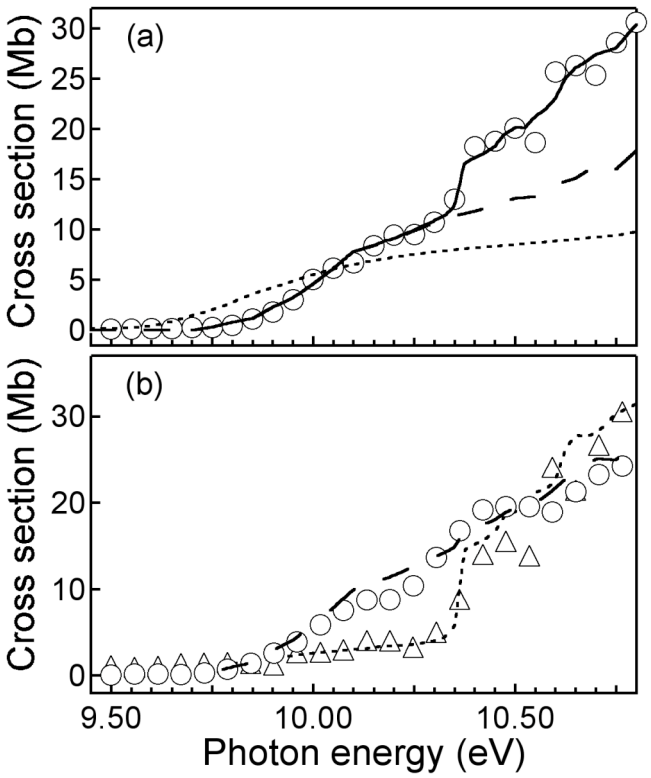
(a)
(b)
Cross section (Mb)
Cross section (Mb)
0
5
10
15
20
25
30
0
10
20
30
9.50
10.00
10.50
Photon energy (eV)

**Figure 5**

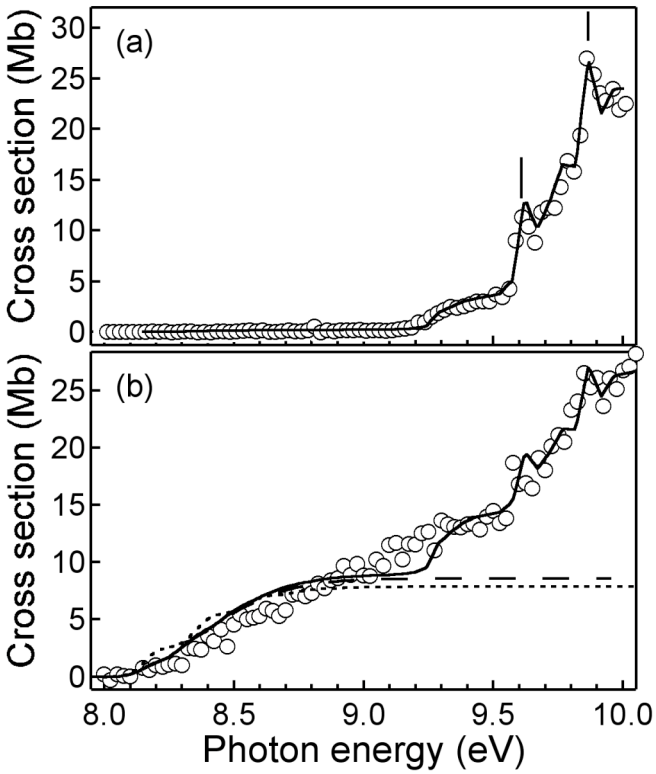
(a)
(b)
Cross section (Mb)
Cross section (Mb)
Photon energy (eV)
0
5
10
15
20
25
30
8.0
8.5
9.0
9.5
10.0

**Figure 6**

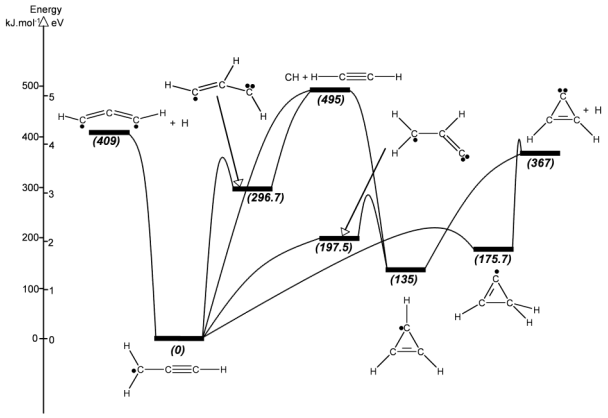
Energy
kJ.mol⁻¹
eV
500
400
300
200
100
0
5
4
3
2
1
0
(409)
(0)
(296.7)
(495)
(197.5)
(135)
(175.7)
(367)
+ H
CH + H—C≡C—H

**Figure 7**

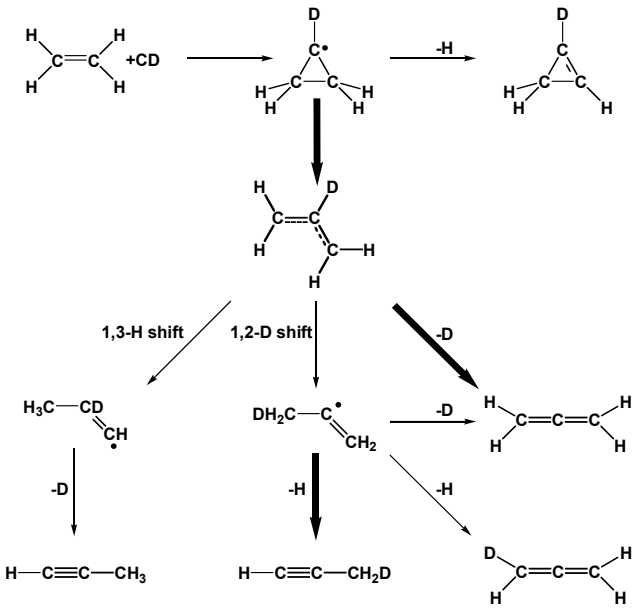

**Figure 8**

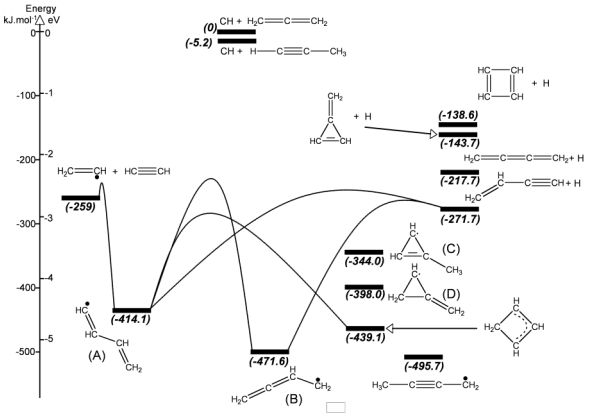
Energy
kJ.mol
eV
0
-100
-200
-300
-400
-500
-1
-2
-3
-4
-5
(0)
(-5.2)
CH + H2C=C=CH2
CH + H-C≡C-CH3
+ H
(-138.6)
(-143.7)
H2C=C=C=CH2 + H
(-217.7)
H2C=CH + HC≡CH
(-259)
(-271.7)
(-344.0)
(C)
(-398.0)
(D)
(-414.1)
(A)
(-439.1)
(-471.6)
(B)
(-495.7)

**Table of contents**